**Supplemental material**

# Long and Very Long Lamellar Phases in Model Stratum Corneum Lipid Membranes

**Running title: Asymmetric Building Unit in Skin Lipid Lamellae**

**Petra Pullmannová[1], Elena Ermakova[2], Andrej Kováčik[1], Lukáš Opálka[1], Jaroslav Maixner[3], Jarmila Zbytovská[1,3], Norbert Kučerka[2,4], Kateřina Vávrová[1]**

[1]Skin Barrier Research Group, Charles University, Faculty of Pharmacy in Hradec Králové, Heyrovského 1203, 500 05 Hradec Králové, Czech Republic

[2]Frank Laboratory of Neutron Physics, Joint Institute for Nuclear Research, Dubna 141980, Russia

[3]University of Chemistry and Technology Prague, Technická 5, 166 28 Prague, Czech Republic

[4]Department of Physical Chemistry of Drugs, Comenius University in Bratislava, Faculty of Pharmacy, Odbojárov 10, 832 32 Bratislava, Slovak Republic

Corresponding author:

Petra Pullmannová, Skin Barrier Research Group, Charles University, Faculty of Pharmacy in Hradec Králové, Heyrovského 1203, 500 05 Hradec Králové, Czech Republic, pullmanp@faf.cuni.cz, Tel.: +420495067638, Fax: +420495067166

**Supplemental table ST1**: The diffraction peak positions of the various phases identified in the presented XRD patterns.

| Sample composition (molar ratio) | Figure | Lamellar phase | | Chol | Region of short-range arrangement |
|---|---|---|---|---|---|
| | | *d* [nm] | Q [$nm^{-1}$] | Q [$nm^{-1}$] | Q [$nm^{-1}$] |
| CerNS24/ FFA(16-24)/ Chol/CholS = 1/1/1/0.13 | 1a | 5.34 (SLP) | 1.19, 2.37, 3.55, 4.72, 7.07, 8.25, 10.60, 11.78 | 1.85<br>3.68<br>11.02 | 15.16<br>16.81 |
| CerNS24/ FFA(16-24)/ Chol/CholS = 1/1/1/0.13 | 1b | 10.64 (MLP) | 1.19, 2.38, 2.99, 3.56, 4.17, 4.74, 5.35, 5.94, 6.54, 7.10, 8.27 | 1.86<br>3.69<br>11.02 | 15.15 |
| CerNS24/ FFA(16-24)/ Chol/CholS = 1/1/1/0.03 | 2a, 4 (dark blue) | 15.90 ($VLLP_{15.9}$) | 1.21, 1.59, 2.02, 2.39, 2.76, 3.19, 3.58, 3.94, 4.38, 4.76, 5.13, 5.54, 5.94, 6.74, 7.13, 7.56, 8.32, 9.50, 10.68, 11.88 | 1.86<br>3.70<br>9.19<br>11.02 | 15.17 |
| CerNS24/ FFA(16-24)/ Chol/CholS = 1/1/1/0.13 | 4 (light blue) | 15.90 ($VLLP_{15.9}$) | 1.23, 1.60, 2.06, 2.40, 2.73, 3.21, 3.59, 3.96, 4.40, 4.77, 5.10, 5.57, 5.95, 6.35, 6.76, 7.14, 7.54, 8.33, 9.51, 10.70, 11.89 | 1.87<br>3.70<br>9.19<br>11.03 | 15.20<br>16.83 |
| | | 21.21 ($VLLP_{21.2}$) | 1.23, 1.53, 2.10, 2.40, 2.71, 3.29, 3.59, 3.88, 4.47, 4.77, 5.09, 5.66, 5.95, 6.84, 7.14, 8.33, 9.51, 10.70, 11.89 | | |
| CerEOS/CerNS24/ FFA(16-24)/ Chol/CholS = 0.3/0.7/1/0.45/0 | 5a | 12.21 (LLP) | 1.08, 1.58, 2.10, 2.61, 3.13, 3.65, 4.16, 4.68, 5.68, 7.25 | 1.87 | 15.22<br>16.85 |

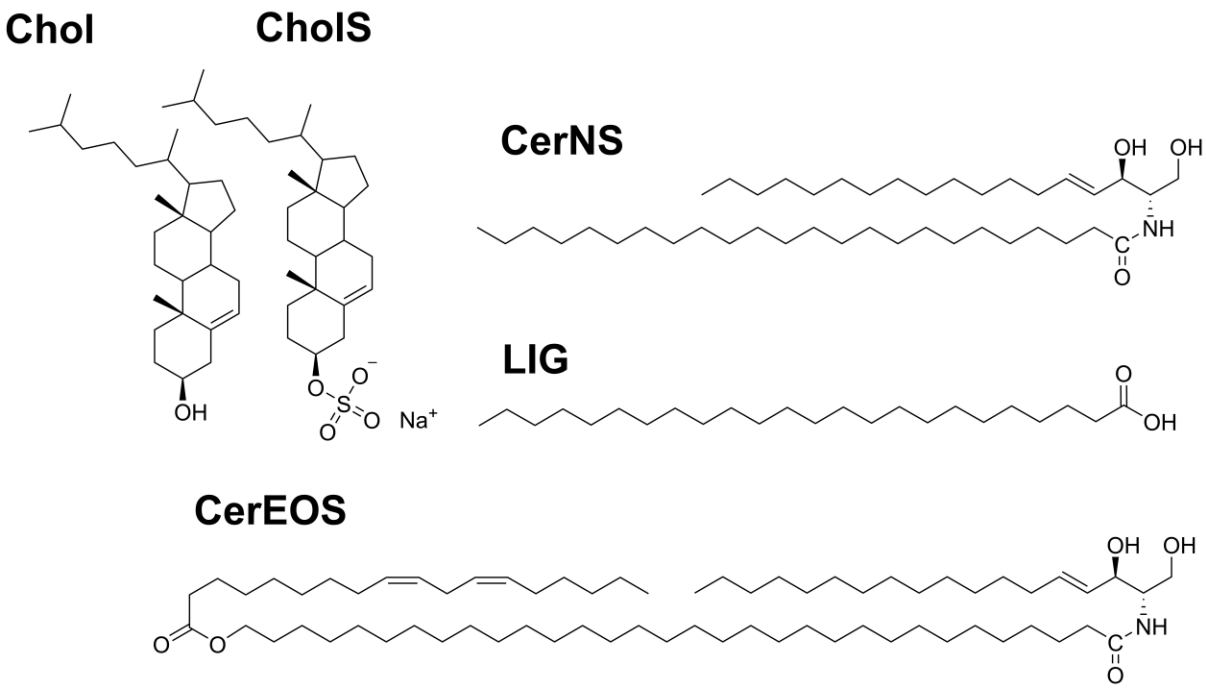


**Supplemental Figure S1: Chemical structures of the lipid components used for the preparation of SC model membranes.** Free fatty acids are represented by lignoceric acid (LIG).

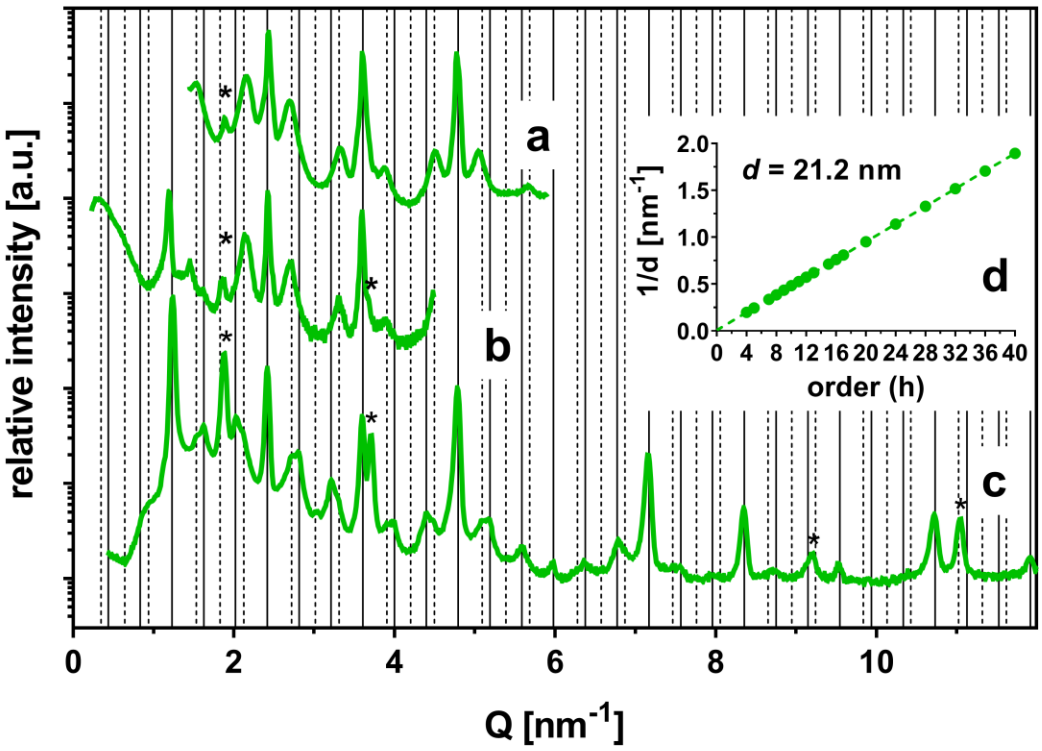


**Supplemental Figure S2: Very long periodicity phases (VLLP) formed in SC model membranes.** XRD pattern of the $VLLP_{21.2}$ formed by the CerNS24/FFA(16-24)/Chol sample (denoted 0.45/0) with the molar ratio Chol/CholS = 0.45/0 after second annealing at 70 °C/$H_2O$ using two different experimental configurations of the diffractometer (**a, b**). XRD pattern of the $VLLP_{15.9}$ and $VLLP_{21.2}$ formed by a control sample with the molar ratio CerNS24/FFA(16-24)/Chol/CholS = 1/1/1/0.13 (denoted 1/0.13) prepared by spraying and annealing at 70 °C/$H_2O$ for 30 min (**c**). Linear regression of the dependence of 1/*d* on the reflection order *h* for $VLLP_{21.2}$ (**d**) of the control sample 1/0.13 depicted in (c). Full grid lines predict the position of $VLLP_{15.9}$ reflections, dashed grid lines predict the positions of selected $VLLP_{21.2}$ reflections. Asterisks indicate the separated cholesterol (Chol); the unscaled intensities are shown in arbitrary units on a logarithmic scale.

**Supplemental discussion of the XRD experiments**

Here we discuss the differences in the intensity distribution (i.e., the relative heights of diffraction peaks) in our XRD spectra in comparison with the spectra measured using other experimental setups. For example, the intensity distribution in the XRD pattern of the short lamellar phase (SLP, $d$ = 5.3 nm) depicted in Figure 1a in the main article differs from the intensity distribution of similar phases published previously (1, 2). These differences are for the most part attributable to the features of experimental setup. The combination of specific sample orientations and the crystallinity, and instrumental geometry of X'pert PRO and Empyrean diffractometers favor higher-Q data while placing a limitation on data below 1 $nm^{-1}$ (although the peak positions could be observed down to ~0.4 $nm^{-1}$). This phenomenon distorts the low-Q intensities presented in our manuscript. Nevertheless, we measured most of the structures presented in the manuscript repeatedly using different experimental setups. To demonstrate the phenomenon discussed, we provide a comparison of patterns that differ in the distribution of intensities yet were obtained from the very same samples or parallel samples (please see Supplemental Figures S3, S4, S5, S6). Please note, that the data discussed herein, those presented in the main article, and the literature data are typically shown in raw format without corrections.

Several factors would have to be taken into account for properly correcting the peak intensities in the measured XRD spectra (3). For example, our measurements utilize a divergence slit programmed for the irradiated length of 20 mm. Thus, the divergence slit is narrow at low angles and wide at high angles. Consequently, the intensity and depth of the incident beam vary. This effect is further intensified at 2theta angles < 2 °. The extremely low incident beam angle in combination with sample characteristics (the orientation and mosaicity of the lamellae, roughness of the sample surface) can cause a loss of peak intensities at low Q in some cases. Also, a substantial part of the beam is absorbed by the sample support at a very low Q. Consequently, most of our measurements did not allow to resolve the low order reflections at the very low angles.

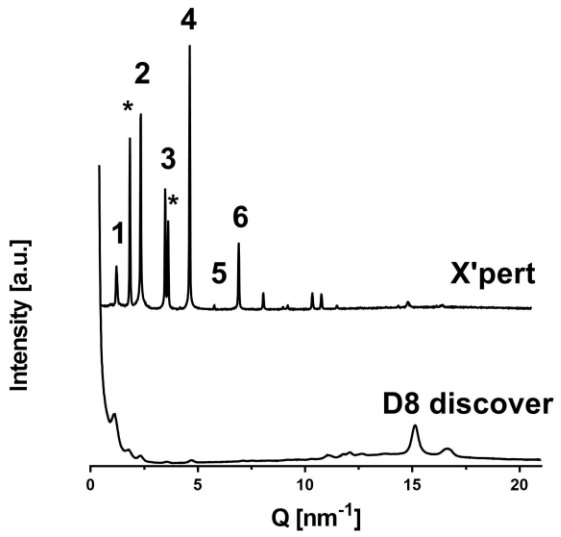


**Supplemental Figure S3:** XRD patterns of the same sample composed of CerNS24/FFA(16-24)/Chol = 1/1/1 (mol/mol/mol) with 5 weight % of CholS ($d$ = 5.3 nm) measured using the X'pert PRO theta-theta diffractometer (PANalytical, Netherlands) and Microdiffraction system D8 Discover (Bruker, Germany) capable of collecting Debye-Scherrer frames (a 2D spectrum was converted into a standard 1D pattern).

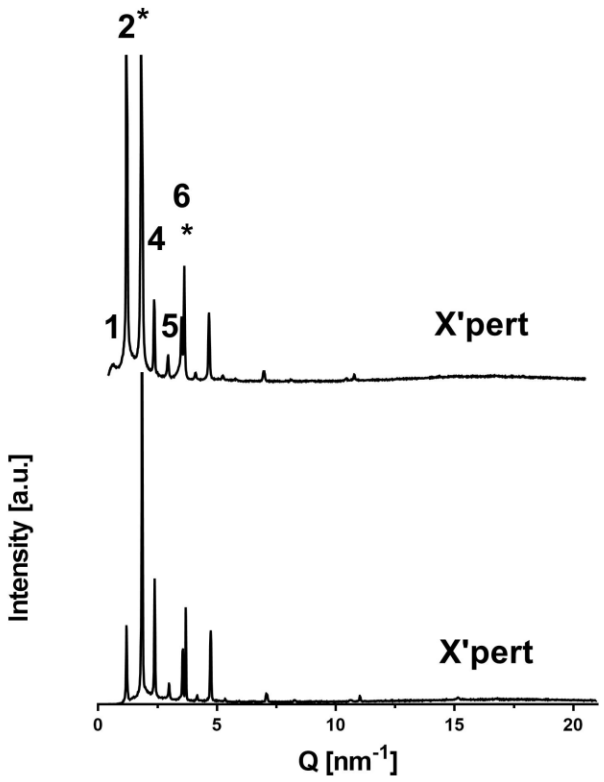


**Supplemental Figure S4:** XRD patterns of parallel samples composed of CerNS24/FFA(16-24)/Chol = 1/1/1 (mol/mol/mol) with 5 weight % of CholS ($d$ = 10.6 nm) measured using the X'pert PRO theta-theta diffractometer.

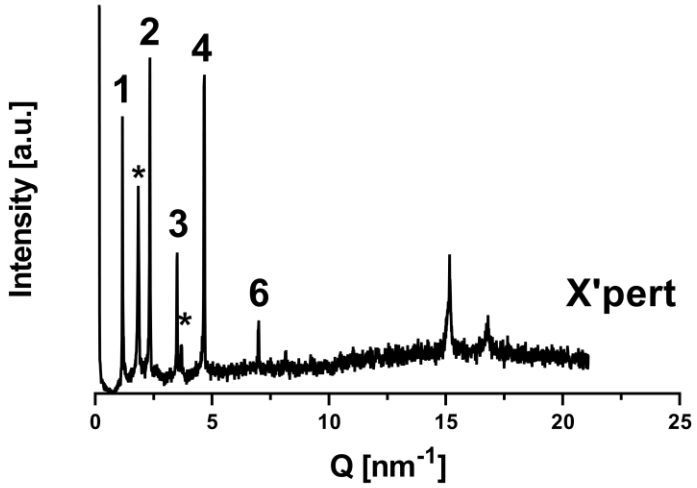


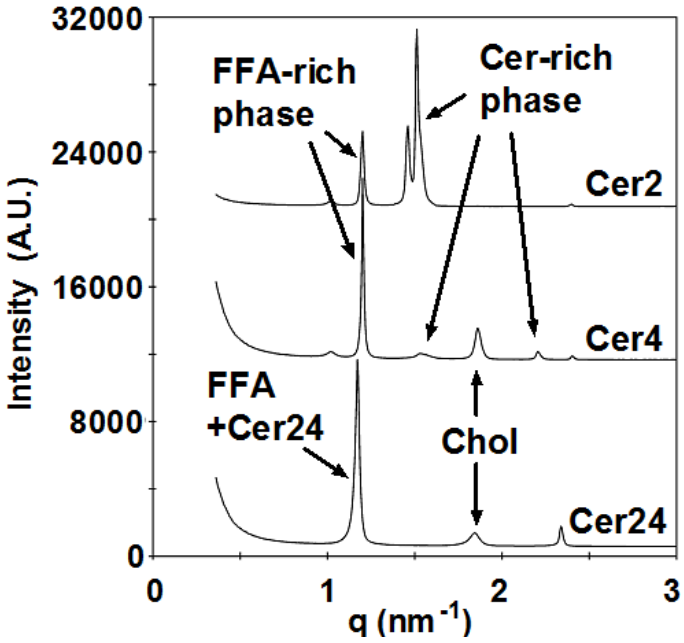


**Supplemental Figure S5:** XRD patterns of parallel samples composed of CerNS24/LIG/Chol = 1/1/1 (mol/mol/mol) + 5 weight % of CholS (d~5.3 nm) measured using the X'pert PRO theta-theta diffractometer (**top**) and synchrotron radiation diffraction (**bottom, Cer24 line**). REPRINTED WITH PERMISSION FROM *ŠKOLOVÁ, B., B. JANŮŠOVÁ, J. ZBYTOVSKÁ, G. GOORIS, J. BOUWSTRA, P. SLEPIČKA, P. BERKA, J. ROH, K. PALÁT, A. HRABÁLEK, AND K. VÁVROVÁ. 2013. CERAMIDES IN THE SKIN LIPID MEMBRANES: LENGTH MATTERS. LANGMUIR. 29: 15624–15633.* COPYRIGHT (2013) AMERICAN CHEMICAL SOCIETY.

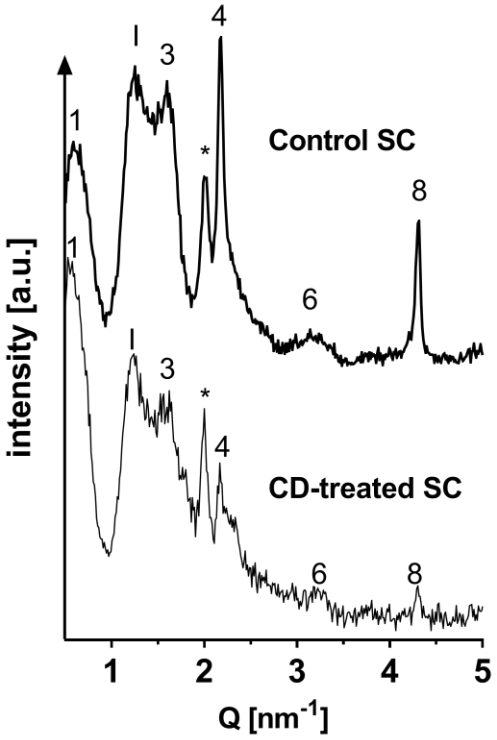


**Supplemental Figure S6:** XRD pattern of isolated stratum corneum (**Control SC**) measured using the X'pert PRO theta-theta diffractometer showing the distortion of intensities at low-Q in comparison to the XRD spectra of SC published in the literature (for example, see (4)). REPRINTED FROM SOCHOROVÁ, M., P. AUDRLICKÁ, M. ČERVENÁ, A. KOVÁČIK, M. KOPEČNÁ, L. OPÁLKA, P. PULLMANNOVÁ, AND K. VÁVROVÁ. 2019. PERMEABILITY AND MICROSTRUCTURE OF CHOLESTEROL-DEPLETED SKIN LIPID MEMBRANES AND HUMAN STRATUM CORNEUM. JOURNAL OF COLLOID AND INTERFACE SCIENCE. 535: 227–238, COPYRIGHT (2019), WITH PERMISSION FROM ELSEVIER.

**REFERENCES**

1. Bouwstra, J. A., G. S. Gooris, K. Cheng, A. Weerheim, W. Bras, and M. Ponec. 1996. Phase behavior of isolated skin lipids. *J. Lipid Res.* **37**: 999–1011.

2. Bouwstra, J. A., G. S. Gooris, F. E. R. Dubbelaar, A. M. Weerheim, A. P. IJzerman, and M. Ponec. 1998. Role of ceramide 1 in the molecular organization of the stratum corneum lipids. *J. Lipid Res.* **39**: 186–196.

3. Xia, Y., M. Li, N. Kučerka, S. Li, and M.-P. Nieh. 2015. In-situ temperature-controllable shear flow device for neutron scattering measurement--an example of aligned bicellar mixtures. *Rev. Sci. Instrum.* **86**: 025112.

4. Bouwstra, J. A., G. S. Gooris, J. A. van der Spek, and W. Bras. 1991. Structural Investigations of Human Stratum Corneum by Small-Angle X-Ray Scattering. *J. Invest. Dermatol.* **97**: 1005–1012.